Variable Antenna Load for Transmitter Efficiency Improvement

Ville Kaajakari, Ari Alastalo, Kaarle Jaakkola, and Heikki Seppä

***Abstract*—A wireless radio transmitter with an integrated variable-impedance antenna is demonstrated. The transmit signal is connected via a switch to the antenna at one of several feed points that correspond to different load impedances that are optimal for the power amplifier at different transmit power levels. It is shown that this can be used to improve the efficiency of the transmission at low and medium transmit powers. The variable antenna load is demonstrated with a planar inverted-F antenna, but the method can be applied to any antenna with suitable impedances.**

***Index Terms*—Antennas, impedance matching, microwave communication, power amplifiers (PAs).**

I. Introduction

THE RF front ends of cellular phones have gone through rapid and continuing integration. This has been driven in part by the change from heterodyne architectures to direct down conversion that allows much of the receiver functionality to be integrated into the baseband signal processor. Another driver has been the integration of discrete components into modules. For example, the front-end switches and surface acoustic wave (SAW) filters are now integrated in the same low-temperature co-fired ceramic (LTCC) package. The benefits of modularization are: 1) reduced packaging costs; 2) reduced design time for a cell phone manufacturer; and 3) smaller final circuitry area. Despite the progress in integration, the antenna essentially remains as an unintegrated industry-standard 50-Ω "black box" to the transceiver designer. In this paper, the efficiency benefits of a variable-impedance antenna integrated as a part of the transmitter are demonstrated.

The power amplifier (PA) consumes a significant amount of the cell phone power budget and considerable effort has been spent in increasing the PA efficiency. Depending on transmission conditions, the output power level of the PA varies from 5 to 33 dBm for global system for mobile communications (GSM) handsets [1]. The PAs are optimized for efficiency at the maximum power level. However, the efficiency falls dramatically when operating at the lower power levels, well below 30 dBm, where the phones are used most of the time [2]. For example, a typical GSM PA efficiency for 20-dBm output power is only approximately 10%. Consequently, there is significant potential for power savings if the amplifier efficiency can be increased at the typically used power levels.

There has been considerable interest in improving the PA efficiency, as this would directly translate to an increase in the operation time of battery-powered portable devices [3]. In general, the amplifiers are classified by their operation point (biasing point). The "class-A" amplifiers conduct current all the time and are thus very linear. The "class-B" and the higher class amplifiers conduct current only during a part of the input cycle and are, therefore, more efficient, but also less linear. There is considerable effort in utilizing schemes such as predistortion to use nonlinear amplifiers in communication systems that require linear signal paths. While these efforts address the demand for the high PA efficiency, they do not directly address the issue of the lowered efficiency at the low transmit power levels.

The PAs reach their maximum efficiency when they operate at the full output voltage swing that normally correspond to the maximum output power. One way to increase the PA efficiency at lower power levels is, therefore, to adjust the dc supply voltage [4]–[6]. This approach increases the efficiency at the low power levels, but the method has two disadvantages, which are: 1) the variable supply requires additional circuit components and 2) the supply voltage conversion suffers from its own conversion losses that lower the overall efficiency also at the maximum power levels.

Another approach to increase the transmitter efficiency at low power levels is to make the matching network between the PA output and antenna adaptive [7][8]. In principle, high efficiencies can be maintained by increasing the matching network impedance. For full benefit, however, the impedance change requirements are quite high. For example, tuning the output by 10 dB requires an impedance adjustment by a factor of ten. In addition, the tunable components need to have low losses and be highly linear to satisfy the spectral purity requirements for wireless communication. These factors have made implementation of tunable matching networks impractical for portable wireless devices.

Methods to increase the transmission efficiency also include an approach to bypass the final stages of the transmitter amplifier for low output powers [9].

Fig. 1(a) shows the solution considered in this paper to increase the PA efficiency at the lower power levels with a minimal increase in the component count. The amplifier is connected through a switch to an antenna that has two different feed points with different impedances. At the lower power levels, the load impedance is increased to maintain full swing of the PA output

Manuscript received January 9, 2007; revised May 8, 2007. This work was supported by Perlos Oyj and Asperation Oy.

V. Kaajakari was with the VTT Technical Research Center of Finland, Espoo FIN-02044 VTT, Finland. He is now with the Institute for Micromanufacturing, Louisiana Tech University, Ruston, LA 71270 USA.

A. Alastalo, K. Jaakkola, and H. Seppä are with the VTT Technical Research Center of Finland, Espoo FIN-02044 VTT, Finland.

Color versions of one or more of the figures in this paper are available online at http://ieeexplore.ieee.org.

Digital Object Identifier 10.1109/TMTT.2007.902093

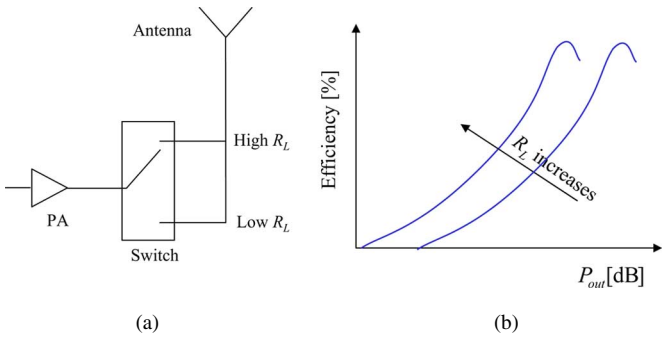

Fig. 1. (a) PA integrated with an antenna that has two different impedance points. (b) By switching between high and low antenna resistances, the power efficiency curve can be adjusted to stay at good efficiencies for all output powers.

voltage that results in good efficiency. Thus, depending on the transmit power level, the power-efficiency curve is adjusted for an overall efficiency increase, as illustrated in Fig. 1(b). To further enhance the control of the efficiency, one can increase the number of feed points, but in this paper, we only consider two feeds for simplicity and because this already captures most of the available power saving.

This paper is organized as follows. In Section II, the concept of using the variable load to increase efficiency at the lower output power levels is verified. This is followed by the demonstrator design and the associated tradeoffs in Sections III and IV. Section V presents the measurement results. Finally, this paper presents discussions and conclusions in Section VI.

II. Simulated Efficiency Improvement

The typical handset PAs are designed to reach their maximum efficiencies of approximately 50% when operated at the full output voltage swing of 3–5 V that correspond to the output power of $P = U^2/R_L$, where U is the output rms voltage and R_L is the load resistance. As the supply voltage is limited by the battery, the cell phone PAs are designed to drive a rather low load resistance typically of 1–4 Ω. This translates approximately to 2 W of maximum RF power, as required by the GSM specifications.

For operation at the lower power levels, the output voltage swing U is reduced, which, unfortunately, also reduces the amplifier efficiency. An alternative way to lower the power is to increase the load impedance R_L, but continuous adjustment is not practical. In this paper, an amplifier topology is proposed that has two discrete load impedances for rough power tuning, while the fine power adjustment is still carried out by adjusting the voltage swing.

To quantify the power savings that are achievable with the variable-load method, PA simulations were done. Fig. 2(a) shows a PA schematic that is based on a typical MESFET transistor [3]. The circuit simulations with different input drive levels and load impedances were carried out using APLAC RF simulation software [10]. The results for two load impedances are shown in Fig. 2(b). As expected, the power efficiency at the low drive levels is better for the higher load impedance. The peak efficiency for the higher impedance is optimized to be at a power level where a significant amount of power is still consumed, but the efficiency of a fixed-load amplifier has

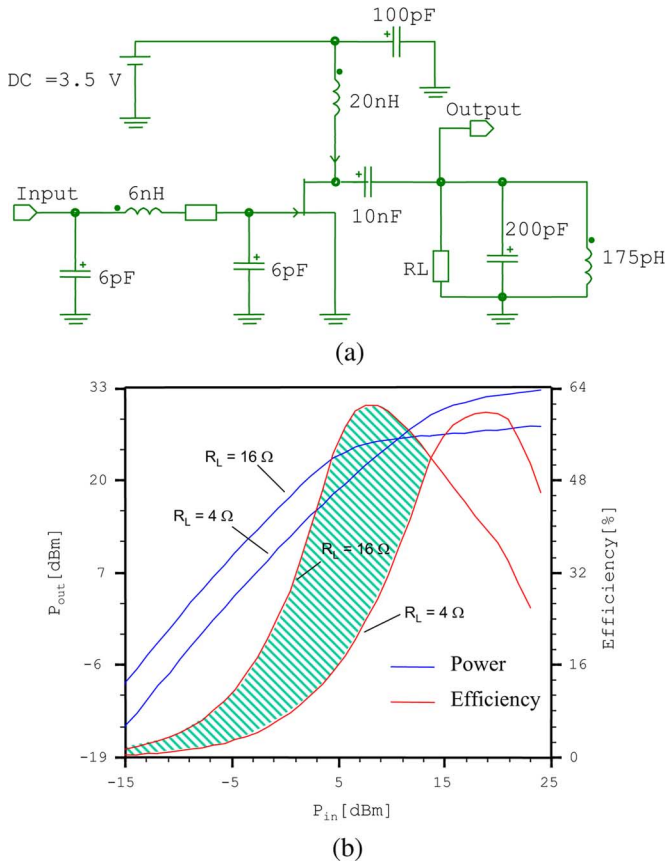

Fig. 2. Simulated RF output power and supply efficiency for two different load impedances. The higher load impedance results in an increased efficiency at the lower output power levels, but also reduces the maximum output power. Shading indicates the region where power savings can be achieved with the variable load impedance method. (a) MESFET PA circuit with ideal load (after [3]). (b) Simulated output power and efficiency.

significantly dropped. The maximum efficiency obtained in the simulations is slightly higher than found for commercial amplifiers due to the idealized tank circuit used in the simulations. The maximum power saving occurs here at approximately $P_{\text{out}} = 24$ dBm where the efficiency is increased from 28% to 60%.

III. Demonstrator Design

Fig. 3 shows the components of the variable load amplifier module. The transmitter consists of: 1) the amplifier; 2) impedance matching element; 3) switch; and 4) antenna with two impedance points. These four elements are covered in Sections III-A–D. The demonstrator was designed for the 869-MHz industrial–scientific–medical (ISM) frequency, which is close to the GSM band.

A. Substrate

The module was implemented on a 3-mm-thick thermoplast substrate that has similar RF properties than polytetrafluoroethylene (PTFE). Fig. 4 shows the cross section of the module. The three-layer module has the ground plane in the middle, electronics on the front surface, and the planar antenna on the back side. The module size was 3.5 cm × 10 cm, approximating the dimensions of a cell phone.

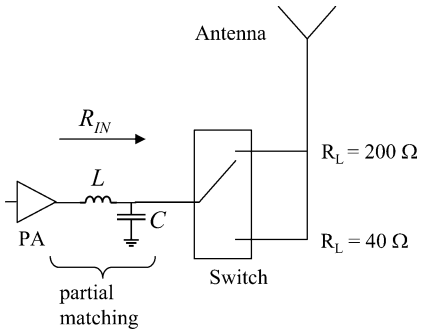

Fig. 3. Components of the variable load amplifier module. Not accounting for matching network and switch losses, the expected shift in the power efficiency curve is 7 dB.

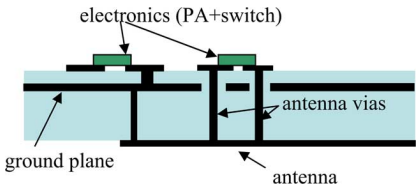

Fig. 4. Cross-sectional view of the demonstrator module that integrates a variable load antenna, switch, and PA.

B. PA

For the PA, the RFMD 2173 from RF Microdevices[1] was chosen. The amplifier is designed for the GSM 900 band and does not contain any impedance-matching elements to 50 Ω in the amplifier chip/module. Thus, the amplifier is well suited for designing the variable-load modules. For the maximum power output, the amplifier should be connected to a $1.5 - j1.7\ \Omega$ load impedance.

C. Impedance Matching

Although the amplifier could, in principle, be directly connected to a 1.5–Ω antenna load, the overall efficiency is increased if higher antenna impedances are used, as this reduces the negative effect of switch losses. For the demonstrator, a simple L-match circuit is used to lower the load impedance seen by the PA.

For the L-match shown in Fig. 3, the transformation ratio is

$$n = \frac{R_L}{R_{\rm IN}} \approx (R_L \omega C)^2 \tag{1}$$

where $R_{\rm IN}$ is the resistance seen by the amplifier, R_L is the (antenna) load resistance, and C is the L-matching capacitance [11]. The approximation in (1) is accurate if $n \gg 1$. As (1) shows, for fixed C, increasing the load resistance R_L *lowers* the PA load $R_{\rm IN}$.

D. Switch

For switching between the antenna loads, a microelectromechanical systems (MEMS) switch (M1C06-CDK2 from Magfusion)[2] was planned to be used. The MEMS switch is based on a direct mechanical contact and, thus, has the advantage of low series resistance leading to small power losses in the switch. However, with the antenna impedance levels of 40 and 200 Ω, a solid-state switch would also have been an alternative.

Unfortunately, the MEMS switch has proven unreliable and failed after a few minutes of testing. The best measurement results were obtained by removing the MEMS switch and directly wiring to the different antenna impedances.

E. Antenna

The antenna that is used in the demonstrator module is a rectangular planar inverted-F antenna (PIFA) [see Fig. 5(a)] implemented on a 3-mm-thick thermoplast substrate. The dimensions of the PIFA are approximately 54.5 mm × 20 mm. The short circuit needed between the actual antenna patch and the ground layer has been realized by a line of vias. The two feed points required to provide the two different feed impedances are easily implemented in the PIFA structure by locating the feed points at different distances from the short-circuiting end of the antenna. As the electronics and radiating antenna element are placed on opposite sides of the ground plane of the module, a signal is fed to the antenna through vias, as shown in Fig. 4. The feed impedance of a (narrow and thin) PIFA has a sine-squared dependency on the distance of the feed point from the short-circuiting end. As the desired feed impedances, i.e., 40 and 200 Ω, are both resistive, the feed points are located symmetrically on both sides of the center line of the antenna patch. This is due to keeping the current distribution around the both feed points as similar as possible. The total distance between the feed points is determined by the distance between the contact pads of the MEMS switch and, therefore, the feed points cannot lie on the center line of the antenna, as would be the ideal case. Tuning of only the real part of the antenna impedance by varying the feed position has also been demonstrated for conventional patch antennas [12]. Fig. 5 shows the simulated radiation pattern. Simulated values for the radiation efficiency and the maximum gain are 62% and 1.9 dBi, respectively.

IV. Design Tradeoffs

The electrical equivalent of the matching and switching circuits is shown in Fig. 6. The matching network losses are modeled with the resistance R_m that determines the unloaded L-match quality factor $Q_m = \omega L/R_m$. To obtain guidelines for optimum design, it is useful to analyze the overall power efficiency from the PA to the antenna. Including the matching and switch losses, the efficiency is

$$\eta = \eta_s \eta_m = \frac{R_L}{R_L + R_S} \cdot \frac{Q_m}{Q_m + \sqrt{n}} \tag{2}$$

where $\eta_s = R_L/(R_L + R_S)$ is the switch efficiency and $\eta_m = Q_m/(Q_m + \sqrt{n})$ is the matching efficiency. Thus, to lower the switch losses due to R_S, high load impedances R_L are required. This, however, translates to a high transformation ratio $n = R_L/R_{\rm IN}$, which will lower the matching efficiency. Therefore, there is an optimal load impedance that will minimize the combined switch and matching-network losses.

As (2) shows, when a single L-match is used for the two different load impedances, optimal design cannot be obtained for

[1]RF Micro Devices Inc., Greensboro, NC. [Online]. Available: www.rfmd.com

[2]Magfusion Inc., Chandler, AZ. [Online]. Available: www.magfusion.com

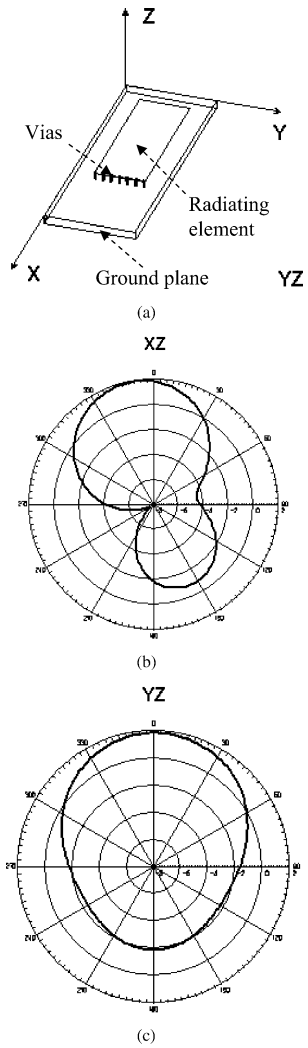

Fig. 5. PIFA antenna and its simulated radiation pattern. (a) PIFA antenna geometry. (b) Simulated radiation pattern in XZ-plane. (c) Simulated radiation pattern in YZ-plane.

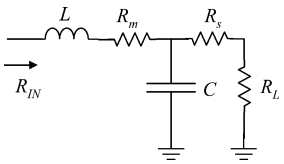

Fig. 6. L-matching network is realized with a transmission line inductance L and a surface mounted 0204 ceramic capacitor C. The switch losses are modeled with a series resistance R_S. The matching network losses are modeled with the resistance R_m that determines the L-tank quality factor $Q_m \gg 1$.

both loads. This will limit the performance of the system if the load impedance is widely varied.

For the demonstrator, antenna loads of 40 and 200 Ω were chosen, as they were easily realized with the antenna. These impedances, however, are rather high and the matching network losses limit the efficiency performance. A more optimal design would have been obtained with lower antenna impedances that could be realized by having the antenna feeds closer to the short circuit. This, however, would have made the impedances much more location sensitive.

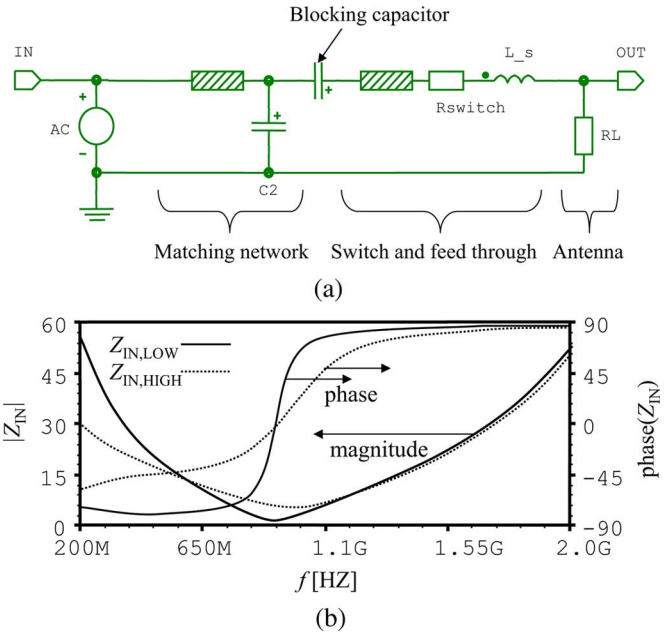

Fig. 7. Simulation of the matching network. (a) Circuit schematic for simulating the PA load impedance and matching network efficiency. (b) Simulated impedance curves (magnitude and phase) for the MEMS switch ($R_S = 0.1\ \Omega$). At the operating frequency, only the real part of the impedance changes when the load resistance is changed.

Fig. 7 shows the circuit schematic for the amplifier load and the simulated $R_{\rm IN}$, as seen by the PA. The series inductance L_s represents the antenna feed through inductance and the switch is modeled with a transmission line and a resistance. The series inductance from the switch and feed through effectively change the circuit topology from an L- to a T-match. The simulated matching-network efficiencies are 74% and 92% for the low- and high-impedance loads, respectively. Accounting for the matching-network losses, the simulated power-efficiency curve difference for the two loads is 5 dB.

V. Measurements

Fig. 8 shows the fabricated demonstrator module. Unfortunately, the MEMS switch failed in the testing and the following measurements were done with the switch removed and manually wiring the two different antenna loads.

The transmitter module efficiencies were measured in pulsed operation (20% duty cycle at 300 Hz), as continuous operation results in heating and loss of PA efficiency. The dc-power consumption was monitored by measuring the amplifier current and voltage during the RF-power-on cycle. In all measurements, the amplifier supply voltage was kept at 3 V. The transmitted RF signal was received with a Suhner antenna and captured using an Agilent Vector Analyzer (89600) in an RF power envelope detection mode. The laboratory measurements were calibrated in an anechoic room where the total radiated power was measured together with the radiation pattern of the antenna. In the antenna measurement, the radiation efficiency of 60% and the maximum gain of 1.7 dBi were recorded. These values correspond well to the antenna simulations.

Fig. 9 shows the measured radiated power and the overall efficiency curves for the manual switch module. The rather low

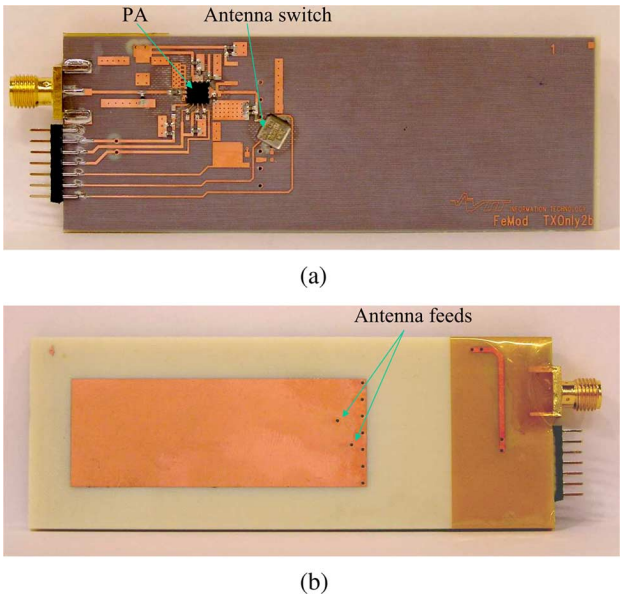

Fig. 8. Demonstrator for the variable-impedance antenna concept. (a) Front side of the demonstrator board showing the PA and switch. (b) Back side of the demonstrator board showing the antenna and feed through locations.

overall transmit efficiency is due to the antenna losses. The efficiency curve with the antenna losses deembedded is shown in Fig. 9(b). The efficiencies are close to 50% for the amplifier and matching network, which is in line with the manufacturer's data sheet for the amplifier. At 25-dBm power output, the obtained efficiency improvement in Fig. 9 was 60% when switching from the low to high load impedance. This magnitude of improvement in PA efficiency can be considered significant.

The obtained 3-dB shift in the efficiency curve correlates well with the simulated shift of 5 dB predicted for 40- and 200-Ω antenna impedances. The 2-dB difference is likely due to a change in internal PA efficiency not accounted for in the simulations. It is well known that due to finite output resistance of PAs, the PA efficiency decreases with decreasing load impedance. Unfortunately, accounting for the change in PA efficiency is not possible, as the load–pull characteristics for the used amplifier are not available.

VI. Discussions

The variable-load antenna was demonstrated to be an effective method for adjusting the PA load impedance. The demonstrated shift of the power-efficiency curve, however, was only 3 dB and the overall efficiency was not optimal. To obtain larger shifts of the power-efficiency curve, the high-to-low impedance ratio should be increased. To obtain a better efficiency, lower antenna impedances should be used. Both goals could be realized by choosing the antenna feed points closer to the PIFA short. As the PIFA impedance follows a $\sin^2$-law, low impedances can be realized. For example, impedances of 10 and 80 Ω would result in a 9-dB shift.

The practical realization of variable antenna with low impedance poses the following challenges.

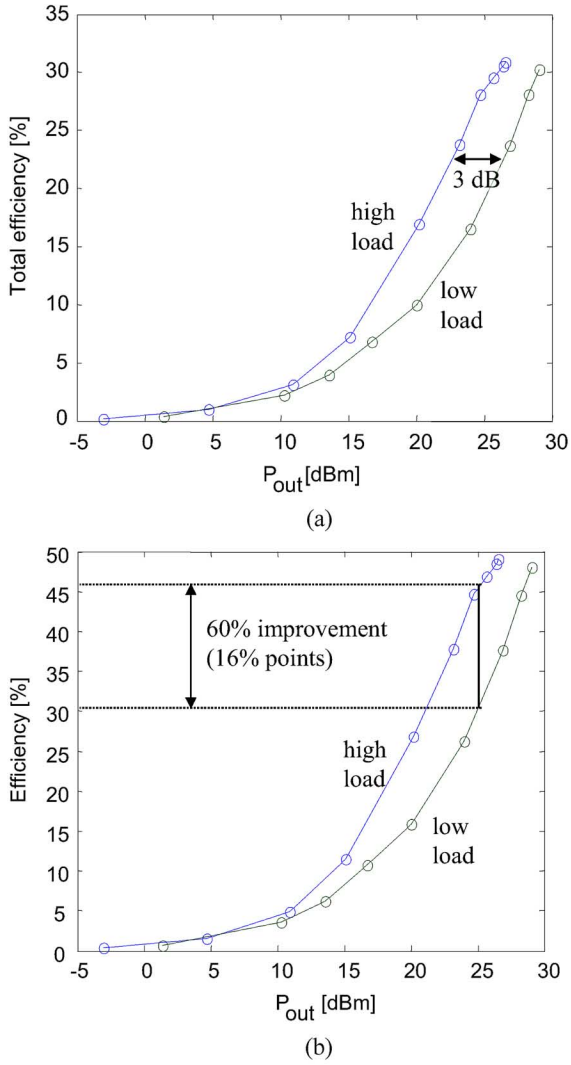

Fig. 9. Measured transmitter efficiencies. (a) Measured overall transmitter efficiency (efficiency from the dc to the transmitted power). The rather low efficiency is due to the antenna losses. (b) Measured efficiency with antenna losses deembedded. The PA efficiency is increased by 60% at 25 dBm when switching from low to high load.

1) Close to the short, the antenna impedance varies rapidly with position and, thus, a good manufacturing precision is needed.
2) Antenna impedance may vary due to external disturbances.
3) The low load impedance requires a low-loss (preferably ohmic) switch.

These challenges are discussed in the following.

The modern circuit board manufacturing enables metal patterns smaller than 100 μm and manufacturing tolerances are of the same order of magnitude. Thus, the first challenge of obtaining sufficient manufacturing tolerances is probably achievable with current technology, although practical realization may require a few design iterations.

The second challenge of antenna impedance variations due to external disturbances is more serious as the cell phone antenna impedance significantly changes due to proximity effects [13]. With the cell phone antenna analyzed in [13], the 40- and 200-Ω antenna impedances would change to $10 + j70$ Ω and

$57 + j400\,\Omega$, respectively, due to a hand being placed close to the antenna. As a result, the simulated impedances seeing by the PA would change from the ideal $0.71 - j1.7\,\Omega$ and $1.5 - j1.7\,\Omega$ to detuned $0.71 - j5.1\,\Omega$ and $0.36 - j2.2\,\Omega$. The significant reduction in the real part of the PA impedance load would reduce the PA efficiency and the radiated power. On a positive note, the proposed variable antenna load is no more susceptible to proximity effects than a single load antenna as both the antenna impedance and matching network follow the traditional design. To battle the large reactive load, two solutions are possible: the variable antenna load may be combined with variable matching/tuning or new additional antenna impedance points may be chosen to provide the desired reactance to counter the environmental variations.

The third challenge of low-loss ohmic switches is both technical and economical. In the demonstrator, the use of a micromechanical switch was planned, but in the end, manual wiring was used due to the reliability problems of the switches. Thus, although all the other components (PA, matching, and antenna) were integrated into a realistic demonstrator, the switching was unrealistic for practical applications. Since the design of the prototype, alternative sources for the micromechanical switches have become available[3,4]. However, it remains to be seen whether the micromechanical switches can be competitive in RF transmitter applications. The solid-state switches are a possible alternative, but due to their higher series resistance, solid-state switches would require higher load impedances to obtain an optimum efficiency. We, therefore, believe that the full benefits of the proposed switchable-antenna load are obtained with micromechanical switches.

VII. Conclusion

A wireless transmitter with an integrated variable-impedance antenna has been demonstrated. By switching between different impedance points of a PIFA antenna, different PA loads have been realized. The PA efficiency has been increased by switching to high load at low transmit power levels. Future work is needed on optimizing the design and improving the switch reliability.

Acknowledgment

The results of this study are based on a collaborative project between the VTT Technical Research Center of Finland, Espoo, Finland, and Perlos Oyj/Asperation Oy, Perlos, Vantaa, Finland.

References

[1] "GSM global system for mobile communications, 3GPP TS 05.01/05.05," ETSI, Sophia-Antipolis, France, 2003.

[2] J. Wiart, C. Dale, A. V. Bosisio, and A. L. Cornec, "Analysis of the influence of the power control and discontinuous transmission on RF exposure with GSM mobile phones," *IEEE Trans. Electromagn. Compat.*, vol. 42, no. 4, pp. 376–385, Nov. 2000.

[3] S. C. Cripps, *RF Power Amplifiers for Wireless Communications*. Norwood, MA: Artech House, 1999.

[4] "Application note 1205," Maxim Integrated Products Inc., Sunnyvale, CA [Online]. Available: www.maxim-ic.com

[5] D. Dening, "Automatic VEE control for optimum power amplifier efficiency," U.S. Patent 6 624 702, 2003, RF Micro Devices Inc., Greensboro, NC.

[6] B. Sahu and G. A. Rincón-Mora, "A high-efficiency linear RF power amplifier with a power-tracking dynamically adaptive buck-boost supply," *IEEE Trans. Microw. Theory Tech.*, vol. 52, no. 1, pp. 112–120, Jan. 2004.

[7] A. Klomsdorf, L. E. Winkelmann, and M. Landherr, "Memory-based amplifier load adjust system," U.S. Patent 6 556 814, 2003, Motorola Inc., Schaumburg, IL.

[8] W. C. E. Neo, Y. Lin, X. D. Liu, L. C. N. de Vreede, L. E. Larson, M. Spirito, M. J. Pelk, K. Buisman, A. Akhnoukh, A. de Graauw, and L. K. Nanver, "Adaptive multi-band multi-mode power amplifier using integrated varactor-based tunable matching networks," *IEEE J. Solid-State Circuits*, vol. 41, no. 9, pp. 2166–2176, Sep. 2006.

[9] J. B. Sung, S. W. Kang, C. H. Hyoung, J. H. Hwang, and Y. T. Kim, "Dual antenna diversity transmitter and system with improved power amplifier efficiency," U.S. Patent Applicat. Publication U.S. 2005/0143024, 2005.

[10] RF Design Tool. APLAC, An AWR Company, Espoo, Finland [Online]. Available: http:www.aplac.co

[11] T. Lee, *The Design of CMOS Radio-Frequency Integrated Circuits*. Cambridge, U.K.: Cambridge Univ. Press, 1998.

[12] L. I. Basilio, M. A. Khayat, J. T. Williams, and S. A. Long, "The dependence of the input impedance on feed position of probe and microstrip line-fed patch antennas," *IEEE Trans. Antennas Propag.*, vol. 49, no. 1, pp. 45–47, Jan. 2001.

[13] K. R. Boyle, Y. Yuan, and L. P. Ligthart, "Analysis of mobile phone antenna impedance variations with user proximity," *IEEE Trans. Antennas Propag.*, vol. 55, no. 2, pp. 364–372, Feb. 2007.

[3]TeraVicta Technologies Inc., Austin, TX. [Online]. Available: http://www.teravicta.com/

[4]WiSpry Inc., Irvine, CA. [Online]. Available: http://www.wispry.com/

Ville Kaajakari received the M.S. and Ph.D. degrees in electrical and computer engineering from the University of Wisconsin–Madison. in 2001 and 2002, respectively.

From 2002 to 2006, he was with the VTT Technical Research Center of Finland, Espoo, Finland, the largest nonuniversity research organization in Northern Europe. While with the VTT Technical Research Center of Finland, he was a Project Manager involved with development of micromechanical reference oscillators. Since 2006, he has been an Assistant Professor with the Institute for Micromanufacturing (IfM), Louisiana Tech University, Ruston.

Ari Alastalo received the M.Sc. and D.Sc. (Tech.) degrees in technical physics from the Helsinki University of Technology, Espoo, Finland, in 1997 and 2006, respectively.

Until 1998, he was involved with magnetic impurities in superconductors. From 1998 to 2002, he was with the Nokia Research Center, where he focused on adaptive-antenna systems. Since 2002, he has been with the VTT Technical Research Center of Finland, Espoo, Finland, where he is currently a Senior Research Scientist leading a team of printable sensors. His research concerns RF components, MEMS, and printable electronics.

Kaarle Jaakkola was born in Helsinki, Finland, in 1976. He received the Master of Science (Tech.) degree in electrical engineering from the Helsinki University of Technology (TKK), Espoo, Finland, in 2003.

Since 2000, he has been with the VTT Technical Research Centre of Finland, Espoo, Finland, initially as a Research Trainee and, since 2003, as a Research Scientist. From 2000 to 2002, he participated in the Palomar (EC IST) Project, during which time he developed RF parts for a new RF identification (RFID) system. His current research interests include RFID systems, wireless and applied sensors, antennas, electromagnetic modeling, and RF electronics.

Heikki Seppä received the M.Sc., Lic.Tech., and Dr.Tech. degrees in technology from the Helsinki University of Technology, Espoo, Finland, in 1977, 1979, and 1989, respectively.

In 1979, he joined the VTT Technical Research Center of Finland, Espoo, Finland, where since 1989, he has been a Research Professor involved with information technology. In 1994, he became Head of the measurement technology field with VTT automation. His research has concerned electrical metrology, in general, and superconducting devices for measurement applications, in particular. He is currently involved with research on dc superconducting quantum interference devices (SQUIDs), the quantized Hall effect, single electron transistor (SET) devices, RF instruments, printable electronics, and microelectromechanical devices.